OPERATING SYNCHROTRON LIGHT SOURCES WITH A HIGH GAIN FREE ELECTRON LASER

S. Di Mitri†, M. Cornacchia, Elettra – Sincrotrone Trieste S.C.p.A., Basovizza, Trieste I-34149

Abstract

The peak current required by a high gain free electron laser (FEL) is not deemed to be compatible with the multi-bunch filling pattern of synchrotrons. We show that this problem can be overcome by virtue of magnetic bunch length compression in a ring section and that, after lasing, the beam returns to equilibrium conditions without beam quality disruption. As a consequence of bunch length compression, the peak current stimulates a high gain FEL emission, while the large energy spread makes the beam less sensitive to the FEL heating and to the microwave instability. The beam large energy spread is matched to the FEL energy bandwidth through a transverse gradient undulator. Feasibility of lasing at 25 nm is shown for the Elettra synchrotron light source (SLS) at 1 GeV. Viable scenarios for the upgrade of existing or planned SLSs to the new hybrid insertion devices-plus-FEL operational mode are discussed, while ensuring little impact on the standard beamlines functionality [1].

CONCEPT

The 260-m long Elettra circumference may internally host a by-pass undulator line ~60 m long at most, with ~20 m left for beam extraction, optics matching to the undulator line and re-injection into the ring. With the one-dimensional (1-D) TGU–SASE model introduced in [2,3], we estimate a saturation length of around 50 m for an FEL radiating at 25 nm, and driven by ~450 A peak current, ~1% relative energy spread beam. The FEL fundamental wavelength is shown in Fig.1-left plot as a function of the beam energy, and defined by the resonance condition $\lambda = (\lambda_u/2\gamma^2)(1 + K^2/2)$, where γ is the relativistic Lorentz factor for the beam energy, λ_u is the undulator period length, $K=eB_0\lambda_u/(2\pi m_e c)$, typically in the range 1–5, is the so-called undulator parameter for a planar undulator, B_0 is the undulator peak magnetic field, e, m_e and c are the electron charge, rest mass and speed of light in vacuum, respectively. The Elettra horizontal equilibrium emittance is shown in the same plot as a function of beam energy ($\varepsilon_x \propto E^2$) and number of dipole magnets in an achromatic cell ($\varepsilon_x \propto 1/N_b^3$; N_b=2 for the actual lattice). At λ=25 nm, the diffraction limit $\varepsilon_x = \lambda/(4\pi) \approx$ 1.8 nm is reached at E=1.0 GeV (see intersection of solid blue and red curve in Fig.1)

We assume to install an S-band RF cavity in a straight section of the ring, and to run it at the phase of zero-crossing. A linear correlation in the electron longitudinal phase space (z,E) is established, and the bunch length is shortened by means of the momentum compaction α_c of the downstream ring section, in our example one half of the Elettra circumference. The following relationship has to be fulfilled by the energy chirp h, the RF peak voltage V, the bunch length compression factor C and $R_{56} = \alpha_c C_R/2$ of half the circumference length C_R:

$$h \equiv \left(\frac{1}{C} - 1\right)\frac{1}{R_{56}} = \frac{1}{E}\frac{dE}{dz} = \frac{2\pi}{\lambda_{RF}}\frac{eV\cos\varphi_{RF}}{E_0 + eV\sin\varphi_{RF}} \approx \frac{\sqrt{\sigma^2_{\delta cor,0} + \sigma^2_{\delta unc,0}}}{\sigma_{z,0}} \quad (1)$$

In Eq. 1, λ_{RF} is the RF wavelength, φ_{RF} (= 0) the RF phase (at zero-crossing), $\sigma_{\delta cor,0}$, $\sigma_{\delta unc,0}$, and $\sigma_{z,0}$, the energy spread correlated with z, the uncorrelated energy spread and the bunch length *before* compression, respectively. In our example, R_{56}=0.21 m, $\sigma_{\delta unc,0}$=0.1% and $\sigma_{z,0}$ =2.7 mm. The chirp that provides minimum bunch length, *i.e.*, maximum peak current at the end of compression is $h = -1/R_{56}$ = -4.8 m^{-1}. The shortest bunch length we can achieve is $R_{56}\sigma_{\delta unc,0}$ = 210 μm, and therefore the maximum effective compression factor is $C = \sigma_{z,0}/(R_{56}\sigma_{\delta unc,0}) \approx 13$. With a bunch charge Q=0.8 nC, a peak current $I = CQc/\left(\sqrt{2\pi}\sigma_{z,0}\right) = 450A$ is provided at the undulator. Linear compression is guaranteed as long as the correlated energy spread is larger than the uncorrelated one; the latter evolves during compression according to $\sigma_{\delta unc} = C\sigma_{\delta unc0}$, because of longitudinal emittance preservation (i.e., the bunch length is shortened by a factor C, whereas the uncorrelated energy spread increases by the same factor). Hence, we require $\sigma_{\delta cor,0} >> \sigma_{\delta unc}$, where $\sigma_{\delta unc} = \sigma_{\delta unc0}$ = 0.1% at equilibrium, and where $\sigma_{\delta unc}$ approaches 1.3% when C→13. At the same time, $\sigma_{\delta cor,0}$ has to be not much larger than the synchrotron momentum acceptance, nominally 3% in Elettra, to avoid particle losses. With the parameters above, Eq.1 specifies $V \approx 76$ MV and $\sigma_{\delta cor,0} \approx$ 1.3%. Fig.1-right plot is the analytical representation of Eq.1, and it suggests that, for any C and $\sigma_{z,0}$, a large R_{56} is desirable to minimize h. A large R_{56}, however, is usually in conflict with the requirement of a low-emittance beam, which is the prerequisite for efficient lasing at short wavelengths.

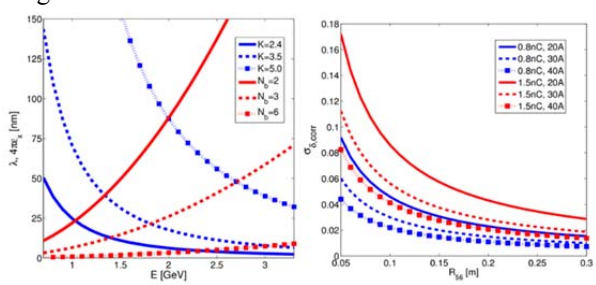

Figure 1: Elettra equilibrium horizontal emittance for different number of dipoles per cell (red), and FEL wavelength for different undulator parameters (blue), vs. beam energy. Right: rms relative correlated energy spread vs. R_{56}, to reach 450 A starting from an initial peak current of 20–40 A. Copyright of NJP (2015) [1].

† simone.dimitri@elettra.eu

After compression is accomplished, the electron beam is directed to an internal by-pass, as shown in Fig.2. The 90 deg extraction arc we consider is a copy of the one introduced in [4], re-adjusted in space for our purposes and enriched by 8 sextupoles to make it achromatic and isochronous, so that bunch length is not affected further. The arc optics is tuned in order to minimize any emittance degradation from coherent synchrotron radiation [1]. Few matching quadrupoles and a small vertical dog-leg at the end of the extraction line prepares the bunch for lasing in the by-pass. A vertical energy dispersion is created by the dog-leg at the level of 2 cm, and it propagates through the vertical TGU in order to ensure lasing even by those electrons far from the resonant energy. The beam is then reinjected into the ring with a transfer line identical, but reversed, to that for extraction, which allows closure of the vertical dispersion. Since the compression has been tuned for an up-right longitudinal phase space at the undulator (minimum bunch length), the reinjected bunch will be decompressed in another half circumference, at the end of which an additional RF structure, identical to the first one, will remove the energy chirp.

ELECTRON BEAM DYNAMICS

The electron beam dynamics is illustrated in Fig.2, where coloured circled labels in the layout correspond to the particle distributions in the other plots of the same Figure (points A–G). Bunch length compression, transport to undulator and de-compression was simulated by tracking 5 million particles with the Elegant code [5], with initial beam parameters of Table 1. There, initial values for the electron beam parameters refer to the equilibrium condition, i.e. before bunch length compression.

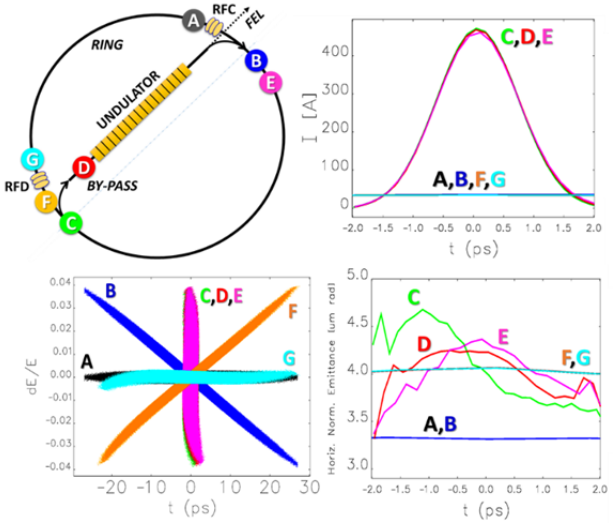

Figure 2: From top-left, clockwise: schematic of synchrotron ring with TGU in by-pass and RF cavities (RFC imposes the energy chirp, RFD removes it); single bunch peak current; slice emittance; longitudinal phase space. A: equilibrium condition. B: energy chirp is added. C: compressed beam. D: entrance of undulator. E: exit of undulator. F: de-compressed beam. G: chirp is removed. Copyright of NJP (2015) [1].

The strengths of 48 sextupoles in the ring were numerically optimized in order to simultaneously ensure: positive linear chromaticities, horizontal dynamic aperture larger than 10 mm at the injection point, ~3% momemtum acceptance, and linear bunch length compression. Tracking results in Fig.2, summarized in Table 1, confirm a beam quality at the undulator suitable for lasing in the ultra-violet wavelength range.

LOW REPETITION RATE SASE FEL

If lasing is done at a rep. rate (RR) smaller than the synchrotron longitudinal damping time, $\tau_s \approx 10$ ms in our example, a bunch is re-injected into the by-pass every time with parameters thermalized to equilibrium, *i.e.*, each FEL pulse is generated like in a single-pass device. The FEL-induced energy spread at saturation is expected to be not larger than $\sigma_{\delta,FEL} = 1.6\rho_{TGU} \approx 0.18\%$ [6], ρ_{TGU} being the TGU-modified FEL parameter [2]. In the one-loop simulation depicted in Fig.2, the effect of lasing was included by adding $\sigma_{\delta,FEL}$ in quadrature to the energy spread of the compressed beam, $\sigma_{\delta unc} \approx 1.3\%$ (point D). The FEL-spent electron beam is close to equilibrium, after de-compression and chirp removal, as shown by the particle distributions at point G in Fig.2. The electron beam vertical emittance is preserved at the 0.02 nm rad equilibrium level, in the assumption of 1% betatron coupling.

The SASE saturation length and the peak power at saturation were evaluated as in the M.Xie 3-D model [7], but now rescaled to the 1-D TGU gain length, $L_{G,TGU}$. Figure 3 shows the single pulse FEL output peak power at λ=25 nm and after a 55 m long undulator, as a function of η_y, and of beam correlated energy spread. $\sigma_{\delta cor,0} = 1.28\%$ allows one to achieve the maximum peak current of 455 A, and 138-MW FEL peak power when $\eta_y = 2.2$ cm. Average betatron functions β_x=20 m, β_y=10 m in the TGU ensure an almost round beam. $L_{G,TGU} = 2.9$ m, and if we arbitrarily enlarge it by 20%, the FEL power lowers to 47 MW.

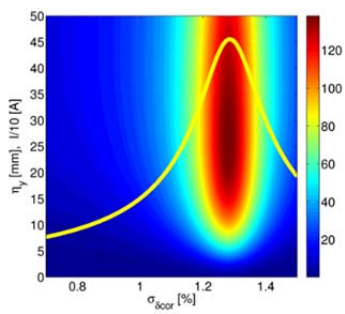

Figure 3: Contour plot of the estimated FEL peak power at saturation in MW *vs.* rms relative energy spread and vertical dispersion in the TGU, for FEL repetition rate ≤ $1/\tau_s \approx 100$ Hz. Maximum power occurs for maximum peak current (yellow solid line). Copyright of NJP (2015) [1].

HIGH REPETITION RATE SASE FEL

We can imagine operating kicker magnets or RF deflectors for a high RR laser production. As an example, RF deflectors enable bunch-by-bunch manipulation. The bunch train will be lasing every 2 turns: after FEL production (point E in Fig.2), half turn is devoted to decompression, one turn and half for providing light to ID beamlines and for returning to the "RF chirper" (point A). After 2 turns, the FEL cycle starts again.

Lasing at RRs higher than $1/\tau_s$ implies *new equilibrium conditions* for the stored beam. These are determined by the simultaneous action of the FEL, which enlarges the beam energy spread at every pass, and the longitudinal damping. We used the algorithm adopted in [8] to evaluate beam current, energy spread and FEL peak power at the new equilibrium, with two important differences: the TGU-modified SASE model is adopted here for the FEL output, and the FEL-induced energy spread is reduced by a factor C due to bunch lengthening after lasing. The modified equation for the *uncompressed* beam's energy spread at the new equilibrium, $\sigma_{\delta,eq}$, reads:

$$\frac{d\sigma_{\delta,eq}^2}{dt} = \frac{\sigma_{\delta inc,0}^2 - \sigma_{\delta,eq}^2}{\tau_s} + \frac{1}{T_{FEL}}\left(\frac{\sigma_{\delta,FEL}}{C}\right)^2 \equiv 0 \qquad (2)$$

Here T_{FEL} is the 2-turns period of lasing, $\sigma_{\delta,FEL}^2 \approx 2\rho_{TGU}P_{FEL}/(eIE)$, $P_{FEL} \approx 0.1P_n \exp(z/L_{G,TGU})$, and P_n the shot noise power of the electron beam at the undulator's entrance [8]. ρ_{TGU} and $L_{G,TGU}$ depend in turn on the beam energy spread at the undulator. ρ is the 1-D FEL parameter [8] and since $\rho \propto I^{1/3}$, with I the peak current *at the undulator*, Eq.2 also takes into account the dependence of I on the energy spread, namely $I = CI_{eq} \propto C\sigma_{\delta,eq}^{-1}$ [9]. The numerical evaluation of $\sigma_{\delta,eq}$ as a function of the undulator length z is shown in Fig.4, together with the peak current at the undulator and the single pulse FEL peak power. The choice of the undulator length can be used to balance FEL power and beam energy spread, in order to tune the operational parameters of the FEL vs. those for the ID beamlines. One should notice that the FEL may also act as a damping wiggler for the transverse emittance at equilibrium. Although generally welcome, this additional effect should be balanced vs. a potential enhancement of intra-beam scattering.

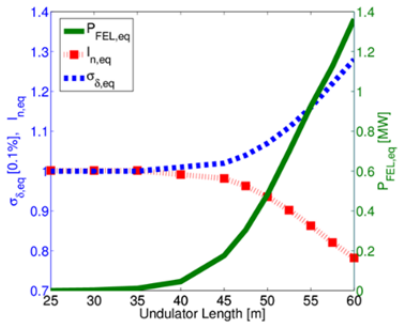

Figure 4: Rms relative energy spread of the uncompressed beam (blue dashed), peak current at FEL normalized to 450 A (red, dotted), and single pulse FEL output peak power (green, solid line), as a function of the undulator length; all parameters are at the *new equilibrium* according to Eq.2, when the FEL RR > 100 Hz. Copyright of NJP (2015) [1].

DISCUSSION

We do not foresee any critical impact of microwave instability on the beam dynamics, because: i) in the low RR FEL scenario, the high single bunch peak current situation lasts for only one turn every damping time, which is not long enough for the instability to build up; ii) the instability current threshold is proportional to the square of the beam energy spread, therefore it "increases" by a factor $C^2 = 169$, when the beam is maximally bunched by a factor C.

Depending on the filling pattern and the duration of the RF pulse in the (de-)chirper cavity, bunches not devoted to lasing may find RF power in the cavity at their passage through it, and thus be subjected to parasitic bunch length gymnastic. In the bunch-by-bunch extraction, that parasitic gymnastic can be avoided, for example, by choosing a pulsed normal conducting cavity whose RF pulse duration is shorter than approximately one revolution period, e.g. ~800 ns. At the same time, the technical challenge of high order mode (HOM) dampers at room temperature should be considered. A superconducting (SC) option for the cavity could alternatively be exploited, for which the HOM dampers technology is now well established. This option, however, implies RF filling times typically not shorter than 1 ms. Finally, in the high RR FEL case, with lasing every few turns, the full compatibility with ID beamlines operation might be solved ab initio by hosting the chirper and de-chirper RF cavities in short by-pass lines parallel to the ring straight sections: only those bunches devoted to lasing will be sent through the cavities by additional fast kicker magnets or RF deflectors.

Table 1: Major Ring and Beam Parameters Used for Tracking

Circumference Length	259.2	m
Harmonic Number	432	
Number of Filled Buckets	≤ 410	
Max. Average Current	380	mA
Longitudinal Damping Time	10	ms
Beam Mean Energy	1.0	GeV
Bunch Charge	0.8	nC
Initial Bunch Duration, RMS	9	ps
Initial Peak Current	35	A
Initial Transv. Emittance, RMS	1.80(x), 0.02(y)	nm
Initial Energy Spread, RMS	0.1	%
S-band RF Peak Voltage	78	MV
Energy Chirp due to RF	-4.8	m^{-1}
R_{56} of Half Circumference	0.21	m
Compression Factor	13	
Bunch Duration at FEL, RMS	0.7	ps
Peak Current at FEL	455	A
Total Energy Spread at FEL	1.3	%
Transv. Emittance at FEL, RMS	2.15(x), 0.02(y)	nm
FEL Fundamental Wavelength	25	nm
Undulator Parameter	2.5	
Undulator Period	46	mm
Undulator Length	55	m
TGU Gradient	65.7	m^{-1}
Vertical Dispersion at FEL	0.022	m
Average Beam Size in TGU, RMS	0.20(x), 0.29(y)	mm

REFERENCES

[1] S. Di Mitri and M. Cornacchia, "Operating synchrotron light sources with a high gain free electron laser," *New J. Phys,.* vol. 17, p. 113006, 2015.

[2] Z. Huang *et al*., "Compact X-ray Free-Electron Laser from a Laser-Plasma Accelerator Using a Transverse-Gradient Undulator*," Phys. Rev. Lett*, vol. 109, p. 204801, 2012.

[3] P. Baxevanis *et al*., "3D theory of a high-gain free-electron laser based on a transverse gradient undulator," *Phys. Rev. ST Accel Beams*, vol. 17, p. 020701, Feb 2014.

[4] D. Douglas *et al*., "Control of Coherent Synchrotron Radiation and Micro-Bunching Effects During Transport of High Brightness Electron Beams", JLAB-ACP-14-1751, March 2014, http://arxiv.org/abs/1403.2318

[5] M. Borland, "elegant: A Flexible SDDS-Compliant Program for Accelerator Simulation," APS Light Source Note LS-287, September 2000.

[6] E.L. Saldin *et al*., "The Physics of Free Electron Lasers", ed. Springer-Verlag, Germany, ISBN 3540662669, p. 62, 2000.

[7] M. Xie, in *Proc. of the 16th PAC*, TPG10, Dallas, TX, 1995.

[8] R. Bonifacio *et al*., "Collective instabilities and high-gain regime in a free electron laser,"*Opt. Commun*., vol. 50, pp. 373–378, 1984.

[9] Z. Huang *et al*., "Steady-state analysis of short-wavelength, high-gain FELs in a large storage ring," *Nucl. Instr. Meth. Phys Research A*, vol. 593, pp. 120-124, August 2008.